

Some Aspects of Finite Length Dipole Antenna Design

P. Banerjee and T. Bezboruah, *Member, IAENG*

Abstract- This paper theoretically investigates current distribution, radiation patterns, directivity, radiation resistance, input impedance, of finite-length dipole antenna using simulation software Matlab-7. Matlab codes are developed for comparison of input impedance and the simulated values are compared with the computed values obtained from numerical methods such as Method of Moments. The simulated values agree with values obtained from numerical methods.

Index Terms – Current distribution, Directivity, Method of Moments, Radiation pattern.

I. INTRODUCTION

In radio and telecommunications a dipole antenna is the simplest and most widely-used class of antenna. Electrical size of antenna is the physical dimension defined relative to wavelength. A finite length dipole is one whose overall dimension is in the range of $3\lambda/2 > l \geq \lambda/2$ [1] (λ = free space wave length) and it's radius a is very thin ($a \ll \lambda$). Yahya et al [1] analyses antenna pattern and gain for different designs of full-wave dipole antenna by changing feed positions. William A. Davis [2] presents the fundamental concepts of wire antenna analysis using modified version of the program Mini-Numerical Electro-magnetics Code(MiniNec) . Branislav M. et al [3] presents a large-domain Galerkin-type Method of Moments (MoM) for the analysis of Electromagnetic (EM) structures composed of arbitrarily excited and loaded dielectric and conducting bodies of arbitrary shapes. The method is based on the integral-equation formulation in the frequency domain. G. K. Avdikos et al [4] demonstrates that the MoM, if well designed and carefully optimized, can be a highly efficient and reliable tool for the analysis and design of a wide class of complex 3-D EM structures. The current distribution, the input impedance and radiation pattern of finite length dipole are also presented in analytical as well as numerical method such as MoM. To get the solutions of Pocklington's integro-differential equation it can be excited by either magnetic frill generator or delta-gap voltage source model. Hallén's integral equation can be solved by only delta-gap voltage source model. In both cases, piecewise constant sub-domain functions and point-matching techniques are used [9]–[12].

Manuscript received March 29, 2014; revised, May 3, 2014.

P. Banerjee is with Department of Physics Jagiroad College, Jagiroad 782410, Morigaon, Assam, INDIA phone: +91-3678-242308 (e-mail: prabirjrd1962@gmail.com).

T. Bezboruah is with the Department of Electronics & Communication Technology, Gauhati University, Guwahati-781014, Assam, INDIA, Fax: +91-361-2700311(O) (e-mail: zbt_gu@yahoo.co.in)

We propose to simulate and study the parameters of finite length dipole like current distribution, radiation pattern, radiation resistance, and directivity in unbound medium. Both, however, use piecewise constant sub-domain functions and point-matching. The program computes the current distribution, normalized amplitude radiation pattern, and input impedance.

II. METHOD OF ANALYSIS:

A. Current Distribution:

For a finite length dipole oriented along z-axis of length l current equation can be represented by [5]:

$$I_e(x', y', z') = \hat{q}_z I_0 \sin\left(k\frac{l}{2} - z'\right), \quad 0 \leq z' \leq \frac{l}{2} \quad (1a)$$

$$I_e(x', y', z') = \hat{q}_z I_0 \sin\left(k\frac{l}{2} + z'\right) \quad -\frac{l}{2} \leq z' \leq 0 \quad (1b)$$

B. Far Zone Electric and Magnetic Field

The expression for total Electric and Magnetic fields of centre-fed finite length dipole antenna given by [5]:

$$E_\theta \approx \frac{j\eta e^{-jkr}}{2\pi r} \left[\left(\cos\left(\frac{kl}{2} \cos\theta\right) - \cos\left(\frac{kl}{2}\right) \right) / \sin\theta \right] \quad (2)$$

$$H_\phi = E_\theta / \eta \quad (3)$$

Where $k = \frac{2\pi}{\lambda}$ (wave number) and $\eta = 120\pi$ (intrinsic wave impedance)

C. Radiation Intensity

The radiation intensity of the dipole may be found as:

$$\begin{aligned} U(\theta, \Phi) &= \frac{r^2}{2} \text{Re}[E_\theta H_\phi^*] \\ &= \eta \frac{|I_0|^2}{8\pi^2} \left[\left(\cos\left(\frac{kl}{2} \cos\theta\right) - \cos\left(\frac{kl}{2}\right) \right) / \sin\theta \right]^2 \quad (4) \end{aligned}$$

D. Directivity

The parameter that is used as a “figure of merit” for the directional properties of the antenna is the directivity and can be written as:

$$D_0 = 4\pi \frac{F(\theta, \Phi)|_{\max}}{\int_0^{2\pi} \int_0^\pi F(\theta, \Phi) d\theta d\Phi} = \frac{2F(\theta, \Phi)|_{\max}}{\int_0^\pi F(\theta) d\theta} \quad (5)$$

Where $F(\theta) = \left[\cos\left(\frac{kl}{2}\cos\theta\right) - \cos\left(\frac{kl}{2}\right) \right] / \sin\theta$ ²
Equation (5) can be rewritten as:

$$D_0 = \frac{2F(\theta, \Phi)|_{\max}}{Q} \quad (5a)$$

Where

$$Q = \left\{ \gamma + \ln(kl) - C_i(kl) + \frac{1}{2} \sin(kl) \times [S_i(2kl) - 2S_i(kl)] + \frac{1}{2} \cos(kl) \times \left[\gamma + \ln\left(\frac{kl}{2}\right) + C_i(2kl) - 2C_i(kl) \right] \right\}$$
(5b)

D. Radiation Resistance, Reactance and Input Resistance and Reactance.

The radiation resistance (R_r) and Input resistance (R_{in}) are given by:

$$R_r = \frac{\eta}{2\pi} \left\{ \gamma + \ln(kl) - C_i(kl) + \frac{1}{2} \sin(kl) \times [S_i(2kl) - 2S_i(kl)] + \frac{1}{2} \cos(kl) \times \left[\gamma + \ln\left(\frac{kl}{2}\right) + C_i(2kl) - 2C_i(kl) \right] \right\}$$
(6)

Where $\gamma=0.5772$ (Euler's constant) and $C_i(x)$ and $S_i(x)$ are cosine and sine integral

$$R_{in} = R_r / \sin^2(kl/2) \quad (7)$$

Similarly reactance can be expressed as:

$$X_m = \eta / 4\pi \{ 2S_i(kl) + \cos(kl) [2S_i(2kl) - S_i(2kl)] - \sin(kl) [2C_i(2kl) - C_i(2kl) - C_i(2ka^2/2)] \}$$
(8)

And input reactance can be written as:

$$X_{in} = X_m / \sin^2(kl/2) \quad (9)$$

E. Pocklington's Integral Equation

Assuming that the wire is very thin ($a \ll \lambda$) Pocklington's integro differential equation [9] can be expressed as [5]

$$\int_{-l/2}^{+l/2} I_z(z') \left[\left(\frac{\partial^2}{\partial z^2} + k^2 \right) G(z, z') \right] dz' = -j\omega \epsilon E_z^i \quad (10)$$

where $G(z, z')$ is Green's function given by:

$$G(z, z') = \frac{1}{2\pi} \int_0^{2\pi} \frac{e^{-kR}}{4\pi R} d\phi' \quad (10a)$$

And

$$R(\rho = a) = \sqrt{4a^2 \sin^2\left(\frac{\phi'}{2}\right) + (z - z')^2} \quad (10b)$$

Where ρ is the radial distance to the observation point and a is the radius.

Eqn.(10) can be used to determine the equivalent filamentary line-source current of the wire, and thus current density on the wire, by knowing the incident field on the surface of the wire. Assuming that the wire is very thin ($a \ll \lambda$) such that (10a) reduces to:

$$G(z, z') = G(R) = \frac{e^{-jkR}}{4\pi R} \quad (10c)$$

We can express eqn.(10) in a more simple form as given in [13]

$$\int_{-l/2}^{+l/2} I_z(z') \frac{e^{-jkR}}{4\pi R^5} [(1 + jkR)(2R^2 - 3a^2) + (kaR)^2] dz' = -j\omega \epsilon E_z^i(\rho = a) \quad (10d)$$

where for observations along the center of the wire ($\rho = 0$)

$$R = \sqrt{a^2 + (z - z')^2} \quad (10e)$$

F. Hallén's Integral Equation

Hallén's integral equation for a perfectly conducting wire given by [5]

$$\int_{-l/2}^{+l/2} I_z(z') \frac{e^{-jkR}}{4\pi R} dz' = -j \sqrt{\frac{\epsilon}{\mu}} [B_1 \cos(kz) + C_1 \sin(k|z|)] \quad (11)$$

If a voltage V_i is applied at the input terminals of the wire, it can be shown that the constant $C_1 = V_i/2$. The constant B_1 is determined from the boundary condition that requires the current to vanish at the end points of the wire.

G. Source Modeling

We have used two methods to model the excitation to represent $E_z^i(\rho = a, 0 \leq \phi \leq 2\pi, -l/2 \leq z \leq +l/2)$ at all points on the surface of the dipole: One is referred to as the (H) delta-gap excitation and the other as the (I) magnetic-frill generator [17].

H. Delta Gap

The delta-gap source modeling is the simplest and most widely used of the two, but it is also the least accurate, especially for impedances. Usually it is most accurate for smaller width gaps. For the delta-gap model, the feed gap Δ is replaced by a narrow band of strips of equivalent magnetic current density given by

$$\mathbf{M}_g = -\hat{\mathbf{n}} \times \mathbf{E}^i = -\hat{\mathbf{a}}_\rho \times \hat{\mathbf{a}}_z \frac{V_s}{\Delta} = \hat{\mathbf{a}}_\phi \frac{V_s}{\Delta}$$

$$-\frac{\Delta}{2} \leq z' \leq \frac{\Delta}{2} \quad (12)$$

I. Magnetic-Frill Generator

In magnetic-frill generator model [17], the feed gap is replaced with a circumferentially directed magnetic current density that exists over an annular aperture with inner radius a , which is chosen as the radius of the wire, and an outer radius b . In our model, the dipole is fed by transmission lines, therefore the outer radius b of the equivalent annular aperture of the magnetic-frill generator is found by using the expression for the characteristic impedance of the transmission line. Over the annular aperture of the magnetic-frill generator, the electric field is represented by the Transverse Electromagnetic (TEM) mode field distribution of a coaxial transmission line given by [5]

$$\mathbf{E}_f = \hat{\mathbf{a}}_\rho \frac{V_s}{2\rho' \ln(b/a)} \quad a \leq \rho' \leq b \quad (13)$$

where V_s is the voltage supplied by the source.

The $1/2$ factor is used because it is assumed that the source impedance is matched to the input impedance of the antenna. The $1/2$ should be replaced by unity if the voltage V_i present at the input to the antenna is used, instead of the voltage V_s supplied by the source. Corresponding equivalent magnetic current density \mathbf{M}_f for the magnetic-frill generator used to represent the aperture is given by[5]:

$$\mathbf{M}_f = -2\hat{\mathbf{n}} \times \mathbf{E}_f = -2\hat{\mathbf{a}}_z \times \hat{\mathbf{a}}_\rho E_\rho$$

$$= -\hat{\mathbf{a}}_\phi \frac{V_s}{\rho' \ln(b/a)} \quad a \leq \rho' \leq b \quad (14)$$

The fields generated by the magnetic-frill generator of eqn.(13) on the surface of the wire is given by [5]

$$\mathbf{E}_z^i(\rho = a, 0 \leq \phi \leq 2\pi, -\frac{l}{2} \leq z \leq \frac{l}{2}) \simeq$$

$$-V_s \left(\frac{k(b^2 - a^2)e^{-jkR_0}}{8\ln(b/a)R_0^2} \left\{ 2 \left[\frac{1}{kR_0} + j \left(1 - \frac{b^2 - a^2}{2R_0^2} \right) \right] + \frac{a^2}{R_0} \left[\left(\frac{1}{kR_0} + j \left(1 - \frac{b^2 + a^2}{2R_0^2} \right) \right) \left(-jk - \frac{2}{R_0} \right) + \left(-\frac{1}{kR_0^2} + j \frac{b^2 + a^2}{R_0^3} \right) \right] \right\} \right)$$

$$(15)$$

$$\text{Where } R_0 = \sqrt{z^2 + a^2} \quad (15a)$$

The fields generated on the surface of the wire is computed using eqn.(14) and can be approximated by [5]

$$\mathbf{E}_z^i(\rho = 0, -\frac{l}{2} \leq z \leq \frac{l}{2})$$

$$= -\frac{V_s}{2\ln(b/a)} \left[\frac{e^{-jkR_1}}{R_1} - \frac{e^{-jkR_2}}{R_2} \right] \quad (15b)$$

$$R_1 = \sqrt{z^2 + a^2} \quad (15c)$$

$$R_2 = \sqrt{z^2 + b^2} \quad (15d)$$

III.METHOD OF MOMENTS

An antenna structure is broken into “segments” and the currents on the segments are then evaluated. The “moment” is numerically the size of the currents times the vector, describing the little segment (length and orientation).

A set of “basis functions” are assumed into which the current distributions are decomposed. The “ MoM” starts from deriving the currents on each segment, or the strength of each moment, by using a coupling Green’s function [14]. This Green’s function incorporates electrostatic coupling between the moments, by knowing the spatial change of the currents, buildup of charges at points on the structure is computed. The MoM was developed by R.F Harrington[6]

IV.RESULTS AND DISCUSSION

We have plotted current distribution eqn.(1a)-(1b) as shown in Fig.1-2 for half-wave and full-wave dipole antenna by using analytical method. The plot of radiation resistance, reactance and input resistance eqn.(6)-(9) is shown in Fig.3-4 for a dipole radius 1.5×10^{-6} m. It can be seen that for small length and radius, input reactance approaches very large value, while for about half wavelength and one and half wavelength dipole antenna, input reactance approaches minimum value. The plot of directivity eqn.(5a) is shown in Fig.5. Number of lobes increases as dipole length increases beyond λ . Maximum directivity is obtained at dipole length 1.25λ . We have compared the results using the two-source modeling (delta-gap and magnetic-frill generator) for Pocklington’s and Hallen’s integral equations, and plotted the variation of the current distribution on a dipole ,as shown in Fig. 6-8 for $l = \lambda/2$ and λ and for dipole radius $a = 1.5 \times 10^{-3}m$ based on the sinusoidal distribution. From the figure it is observed that current is zero at the centre which implies an infinite impedance, in actual antenna design; the impedance is not infinite but is very large value. The results of input impedance calculated by numerical method integral equation solution is listed in the Table-1 also directivity calculated for different length of dipole antenna in linear and decibel scale (dB) is listed in Table-2 below. It can be seen that Hallén’s method excited by delta gap source gives fairly accurate result of input impedance, for moderate number of segments. While Pocklington’s magnetic frill method gives good approximation of input impedance for very high value of sub-sections. Plot of 3-D and 2-D Radiation pattern is shown in Fig.9-12. It is apparent from the plot that number of lobes increases as length of the dipole increases beyond λ .

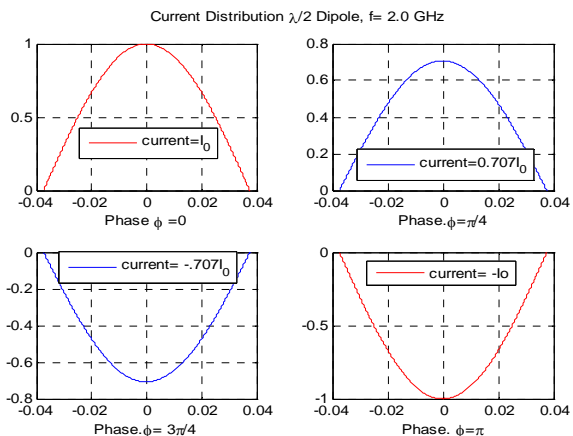


Fig-1 Current for $\lambda/2$ length dipole (phase $\Phi=0, \frac{\pi}{4}, \frac{3\pi}{4}$ and π)

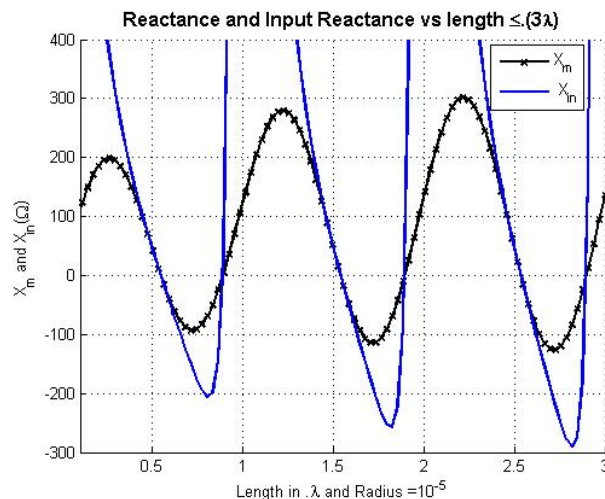


Fig.3 Plot of X_m and X_{in} for dipole antenna ($l \leq 3\lambda$)

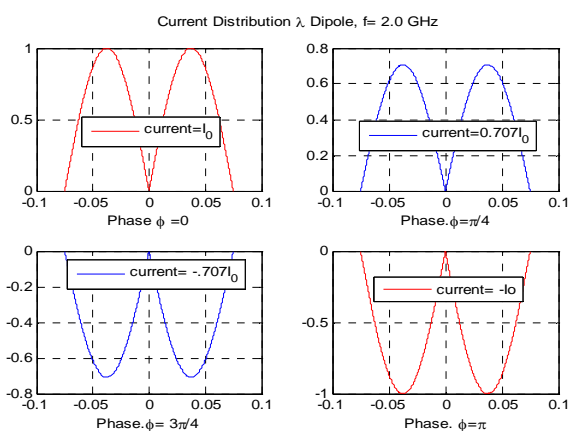


Fig-2 Current for λ length dipole (phase $\Phi=0, \frac{\pi}{4}, \frac{3\pi}{4}$ and π)

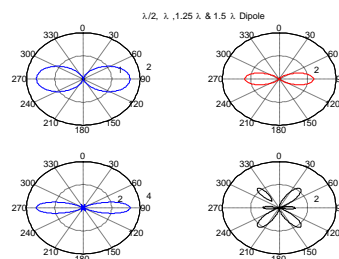


Fig.5 Directivity plot for $\lambda/2, \lambda, 1.25\lambda$ and 1.5λ length dipole

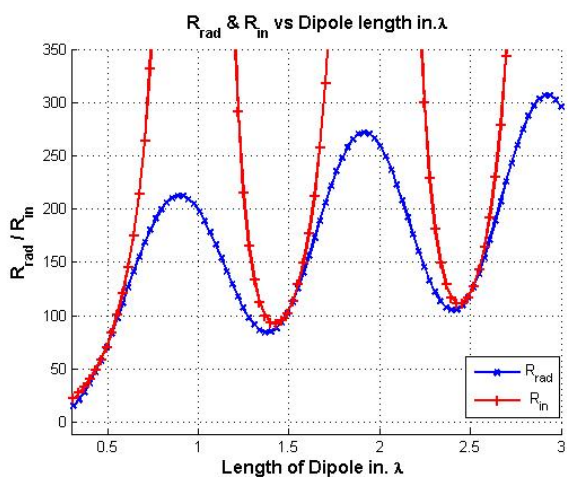


Fig.3 Plot of R_{rad} and R_{in} for dipole antenna ($l \leq 3\lambda$)

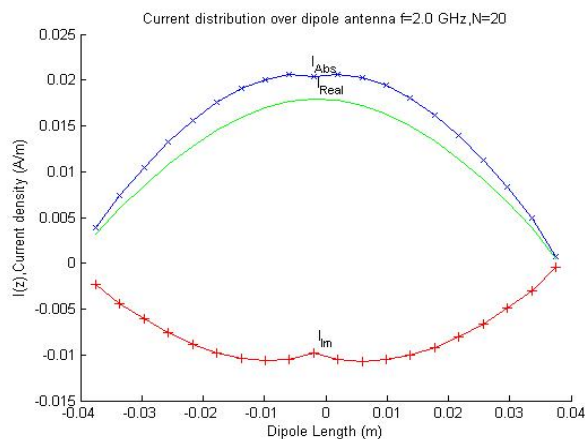


Fig-6 Current for $\lambda/2$ length dipole using Hallen's equation delta gap method

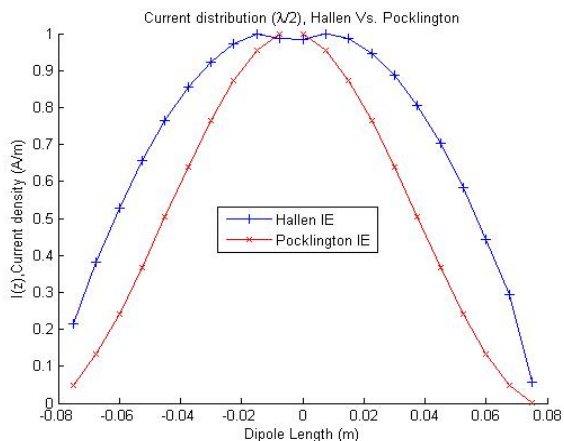


Fig-7 Current for $\lambda/2$ length dipole using Hallen's and Pocklington's dela gap method

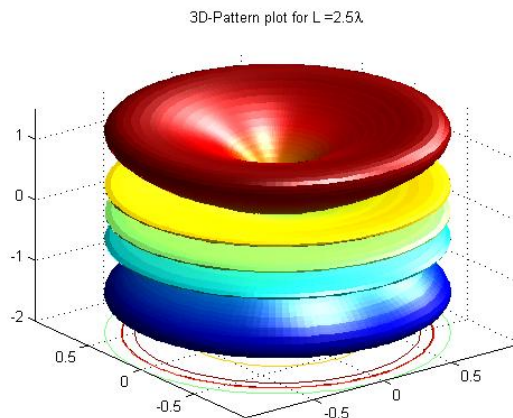


Fig-10 3-D Radiation Pattern of $\lambda/2$ length dipole Antenna

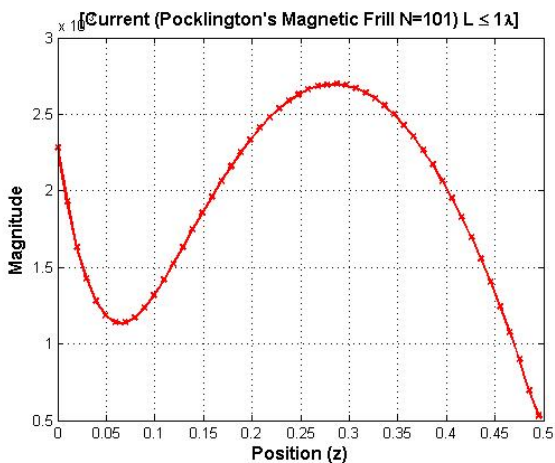


Fig-8 Current for 1.0λ length dipole using Pocklington's equation Magnetic Frill generator no of segments $N=101$.

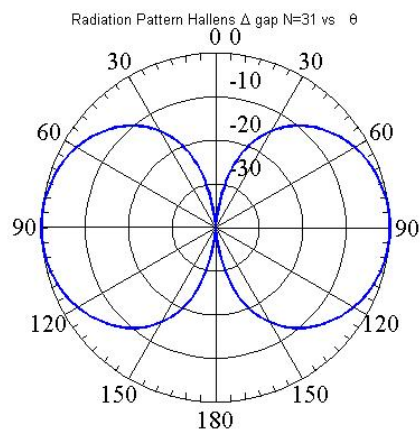


Fig-11 Radiation Pattern of $\lambda/2$ length dipole Antenna

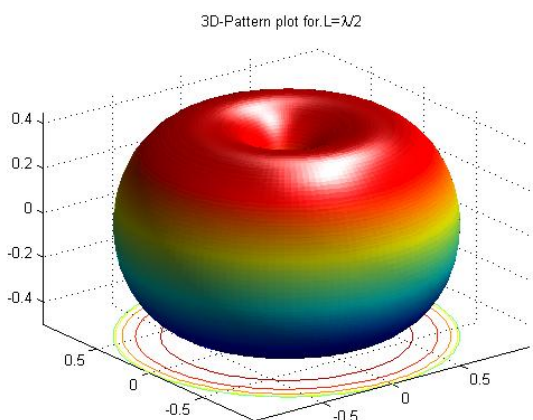


Fig-9 Radiation Pattern (3-D) of $\lambda/2$ length dipole Antenna

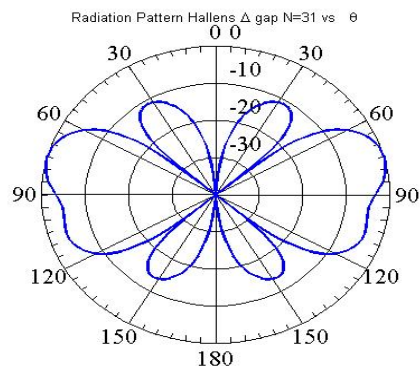


Fig-12 2-D Radiation Pattern of 1.5λ length dipole Antenna

Table-1 Comparisons of Input Impedance

Seg. No	Dipole Length in λ	Radius in λ	Input Impedance (Ω) by Delta Gap Voltage (Hallén's Equation)	Input Impedance (Ω) by Delta Gap Voltage (Pockington Equation)	Input Impedance (Ω) by Magnetic-Frill (Pockington Equation)	Eqn.(7) & (8)
51	0.5λ	0.01λ	$124.3 - j 7.5$	$128.4 + j 25.9$	$110.0 + j 50.7$	$73.1 + j 42.5$
31	--do--	--do--	$108.5 + j 27.4$	$112.5 + j 36.3$	$102.4 + j 43.1$	
51	0.48λ	--do--	$71.9 - j 0.2$	$80.1 + j 33.3$	$24.8 + j 10.3$	$64.73 + j 62.6$
81	--do--	--do--	$73.1 + j 3.8$	$74.3 - j 0.6$	$35.5 - j 0.3$	
51	--do--	0.005λ	$82.6 + j 15.6$	$83.4 + j 14.$	$78.1 + j 15.3$	
51	λ	0.01λ	$139.7 - j 314.0$	$193.9 - j 359.1$	$281.2 - j 383.7$	$199.1 + j 125.4$
31	λ	0.01λ	$223.2 - j 371.0$	$298.7 - j 411.0$	$277.8 - j 325.5$	
101	λ	--do--	$34.3 - j 167.3$	$72.0 - j 237.4$	$224.6 - j 375.5$	
101	1.5λ	--do--	$145.5 + j 6.5$	$143.1 + j 13.2$	$134.6 + j 30.1$	$105.5 + j 45.54$
31	1.5λ	--do--	$116.3 + j 13.4$	$128.9 + j 4.6$	$73.2 + j 3.7$	
51	1.5λ	--do--	$128.6 + j 18.9$	$120.2 - j 11.5$	$97.0 - j 6.0$	

[8]. Robert W. Schuler, "A Study of Dipole Antennas using MatLab", The Catholic University of America, 2003, pp-1-44.

Table-2 Comparisons of Directivity (in linear scale and dB)

Length of Dipole	Directivity (dimension less)	Directivity (dB)
$\lambda/2$	2.1509	1.641
λ	3.822	2.41
1.25λ	5.1621	3.28
1.5λ	3.4757	2.32

V. CONCLUSION

We have graphically represented current distribution, radiation resistance, reactance, input resistance and reactance and directivity of finite length dipole at far field region. We have used Pocklington's integro-differential equation and Hallén's integral equation to find the current distribution on conducting wires, and then the values of input impedance obtained from two methods are compared. In all the cases theoretical results are found to be closely agrees with the experimental results.

References

[1]. Yahya S. H. Khraisat, Khedher A. Hmood, Anwar Al-Mofleh, "Analysis of the Radiation Resistance and Gain of Full-Wave Dipole Antenna for Different Feeding Design", Journal of Electromagnetic Analysis and Applications, 2012, 4, pp. 235-242

[2]. William A. Davis, "Numerical Methods for Wire Structures", Virginia Polytechnic Institute and State University, March 1995, pp.1-11.

[3]. Branislav M. Notaro's Branko D. Popovic', Jan PeetersWeem, Robert A. Brown, and Zoya Popovic', "Efficient Large-Domain MoM Solutions to Electrically Large Practical EM Problems", IEEE Transactions on Microwave Theory and Techniques, Vol. 49, No. 1, January 2001, pp.151-159.

[4]. G. K. Avdikos, H. T. Anastassiou, "Computational Complexity of the Moment Method for Various Matrix Calculation Schemes", URSI EMTS, 2004, pp.1137-1139

[5]. Constantine A. Balanis, Antenna Theory, John Wiley & Sons, Inc., 3rd ed., ISBN 978-81-265-2422-8, 2005, pp.434-459

[6]. Harrington, R.F., Field Computation by Moment Methods, MacMillan, New York, USA, 1968.

[7]. R. E. Burgess, "Aerial Characteristics," Wireless Engr., Vol. 21, April 1944, pp. 154-160.

[9]. H. C. Pocklington, "Electrical Oscillations in Wire," Cambridge Philos. Soc. Proc., Vol. 9, 1897. pp. 324-332.

[10]. E. Hall'en, "Theoretical investigations into the transmitting and receiving qualities of antennae," Nova Acta Regiae Soc. Sci. Upsaliensis, Ser. IV, No. 4, , 1938, pp. 1-44.

[11]. R. King and C. W. Harrison, Jr., "The distribution of current along a symmetric center driven antenna," Proc. IRE, Vol. 31, October 1943, pp. 548-567.

[12]. J. H. Richmond, "A Wire-Grid Model for Scattering by Conducting Bodies," IEEE Trans. Antennas Propagat. Vol. AP-14, No. 6, November 1966, pp. 782-786.

[13]. G. A. Thiele, "Wire Antennas," in Computer Techniques for Electromagnetics, R. Mittra (Ed.), Pergamon, New York, Chapter 2, 1973, pp. 7-70.

[14]. L. W. Pearson and C. M. Butler, "Inadequacies of Collocation Solutions to Pocklington-Type Models of Thin-Wire Structures," IEEE Trans. Antennas Propagat., Vol. AP-23, No.2, March 1975, pp. 293-298.

[15]. C. M. Butler and D. R. Wilton, "Analysis of Various Numerical Techniques Applied to Thin-Wire Scatterers," IEEE Trans. Antennas Propagat., Vol. AP-23, No. 4, July 1975, pp. 534-540.

[16]. D. R. Wilton and C. M. Butler, "Efficient Numerical Techniques for Solving Pocklington's Equation and their Relationships to Other Methods," IEEE Trans. Antennas Propagat., Vol. AP-24, No. 1, January 1976, pp. 83-86.

[17]. L. L. Tsai, "A Numerical Solution for the Near and Far Fields of an Annular Ring of Magnetic Current," IEEE Trans. Antennas Propagat., Vol. AP-20, No. 5, September 1972, pp. 569-576.

Date of modification: 3 May, 2014

Abstract: First line "and graphically" omitted, underline and fontsize of "radiation resistance" changed, comma after "input impedance" omitted, "finite-length dipole antenna", "s" omitted, MoM, omitted

Introduction: "MoM" replaced by Method of Moments, EM replaced by Electromagnetic.

Conclusion: Third line "relation" omitted, Last four lines omitted